

Application Achievements through Usuda Deep Space Center and Associated Control System

July 7, 2024

ISAS

MitsubishiElectricCorporation

NEC

(Proposers: Tadashi Takano and Yashiro Murata)

Listed missions and observations

- Voyager2 in Neptune encounter
- Bistatic Radar System: Detecting Space Debris
- Hayabusa: asteroid explorer
- Kaguya family including Oona and Okina: Lunar probe
- Venus Express and Akatsuki: Venus explorers
- Hayabusa: asteroid explorer

Voyager2 in Neptune encounter

1992 Voyager Radio Science_e75-b_7_665

a of the signal around the multipath region,
ing the Canberra 8.4 GHz data after remov-
t of $(f_{\text{pred}} - f_{\text{tun}})$ (corresponding to Fig. 3
aining gradual frequency drift, especially
20, is due to $f_{\text{unmodelled}}$.

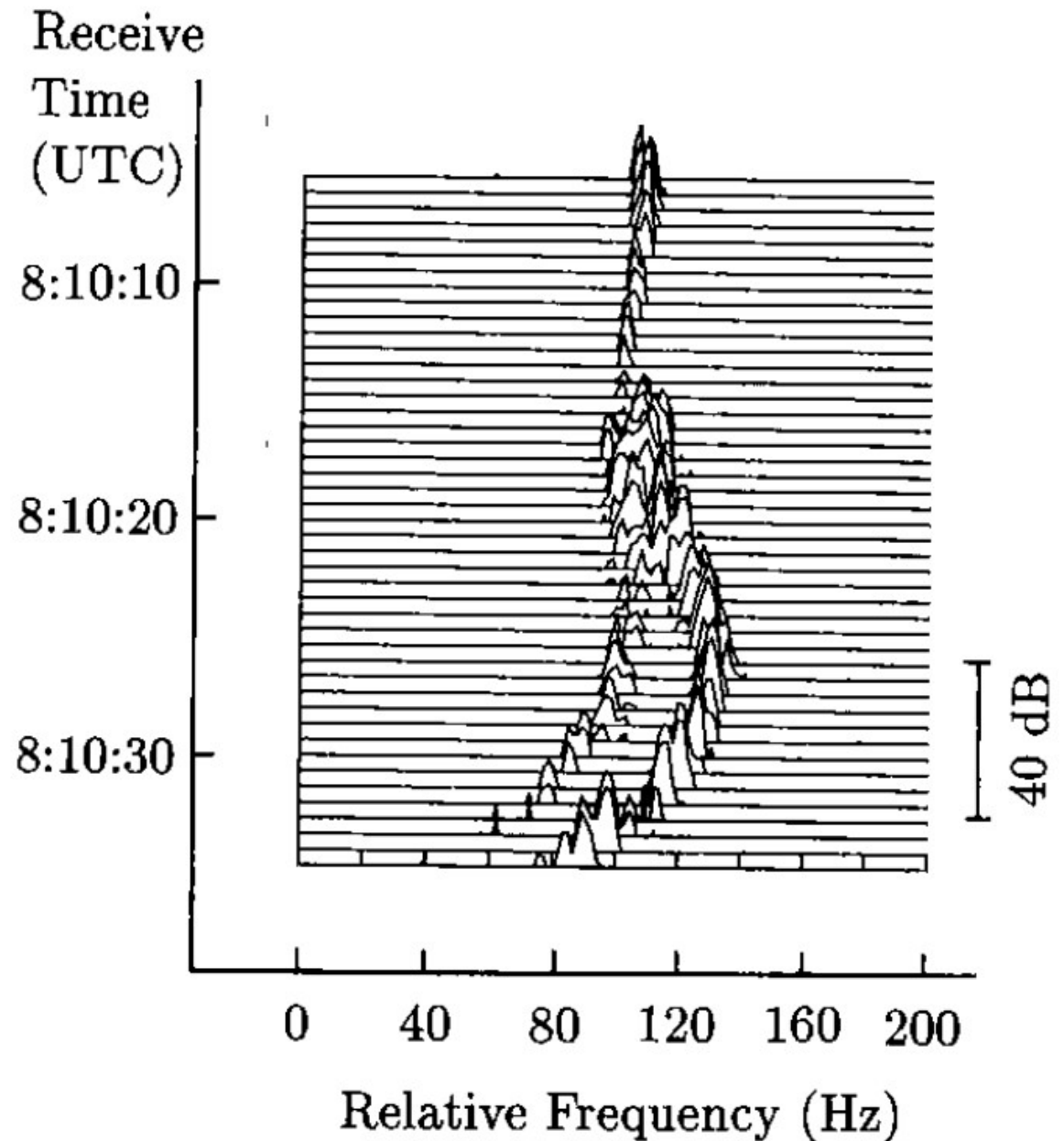


Fig..

Bistatic Radar System for Detecting Space Debris

Yajima, Earth, Moon, and Planets (2007)

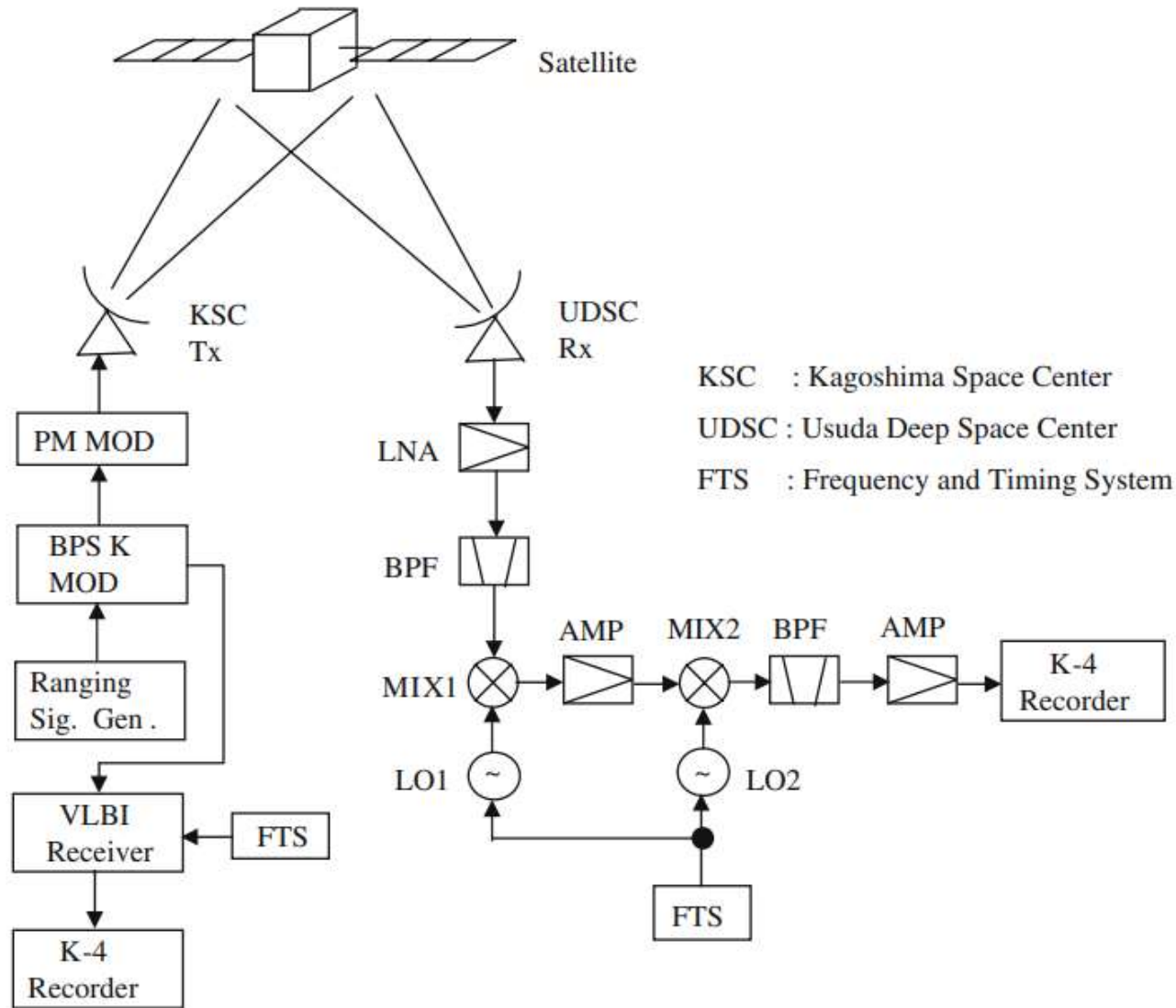


Figure 4. Configuration of the experimental system.

Hayabusa

2015Yoshikawa_Hayabusa_sample return mission

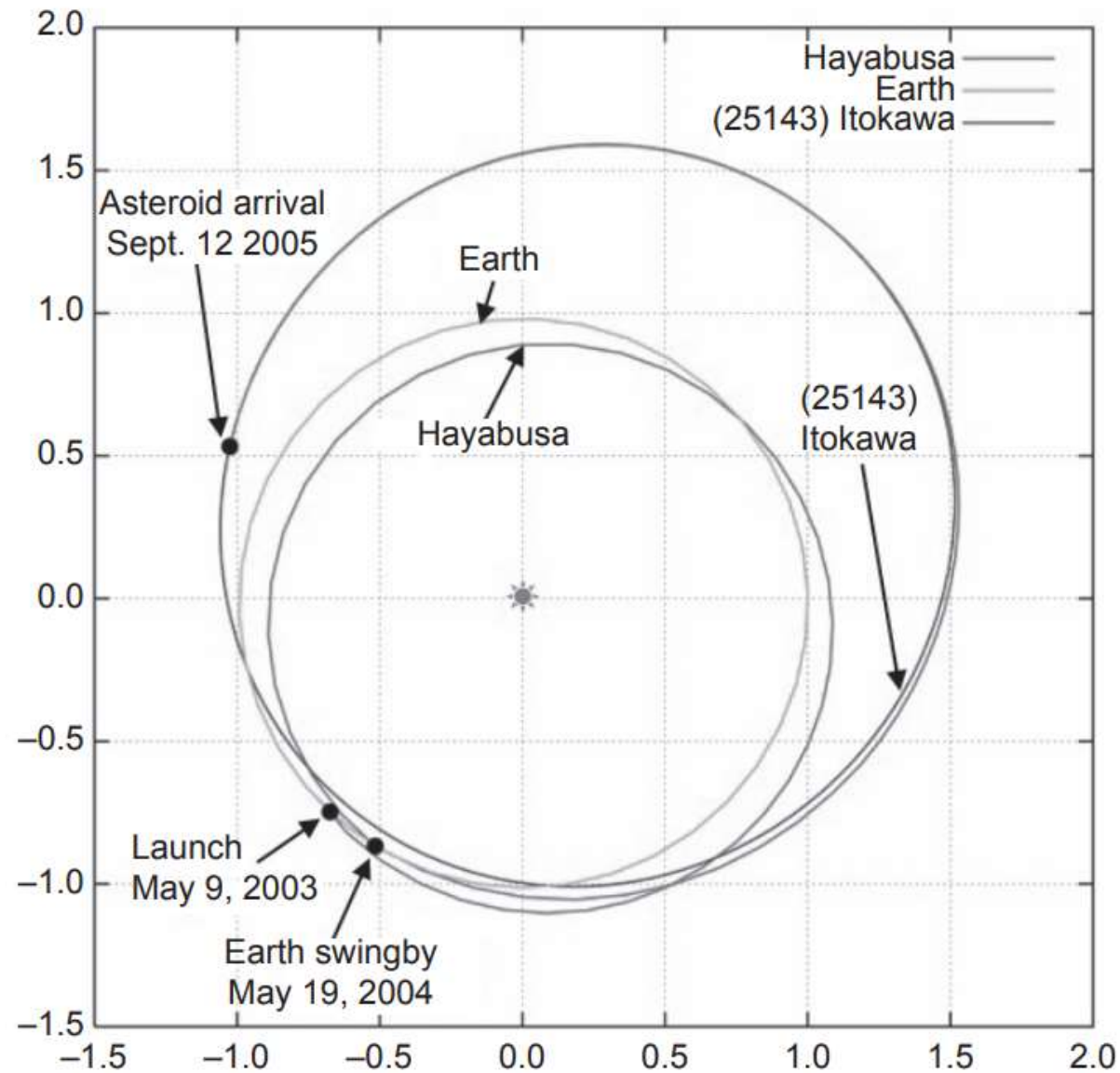


Fig. 1. Orbit of Hayabusa from launch to asteroid arrival. The EDVEGA phase was from launch to Earth swingby, and the transfer phase was from Earth swingby to asteroid arrival.

Hayabusa

2006Yano Touchdown of the Hayabusa Spacecraft at

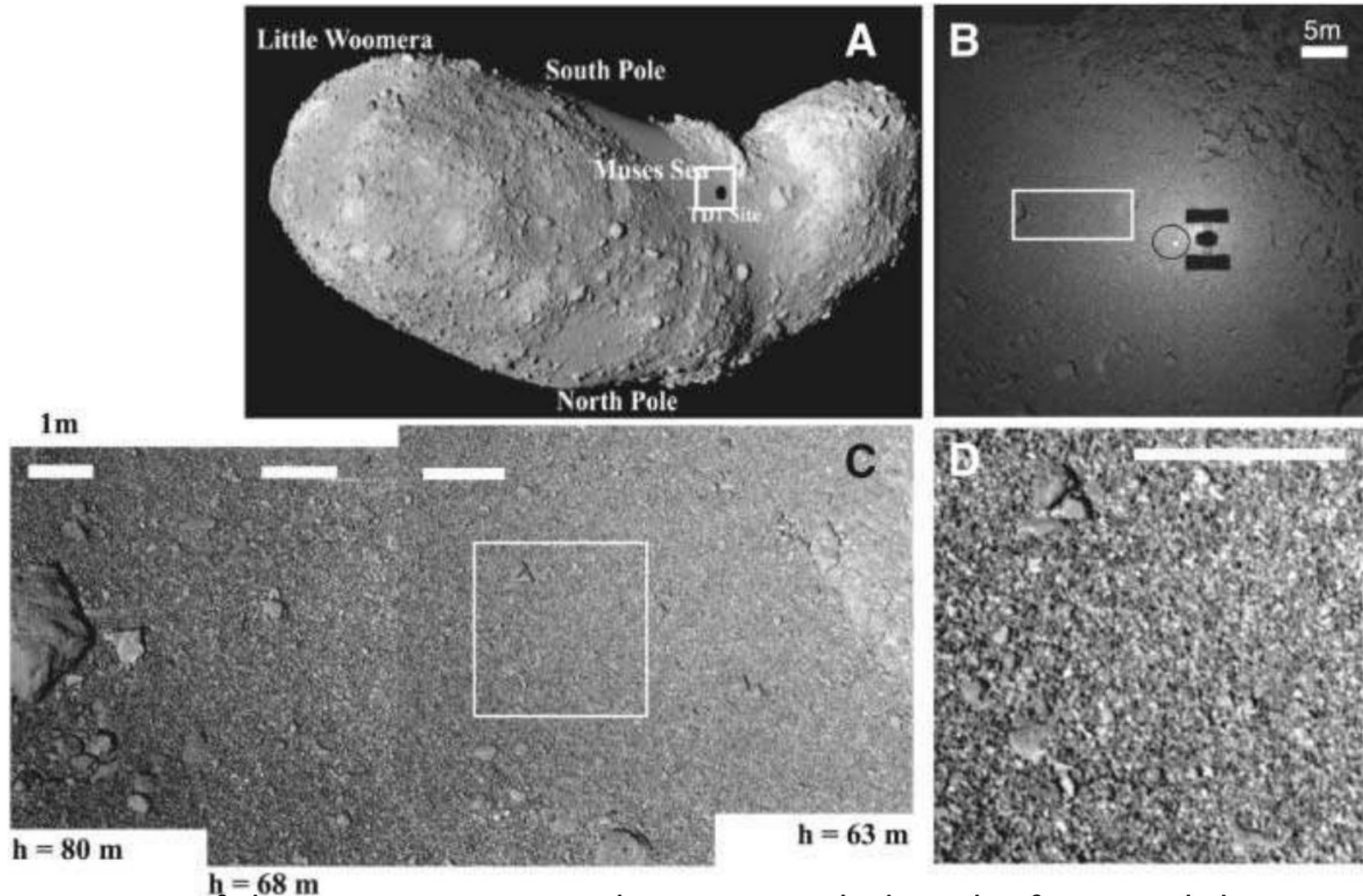


Fig. 1. Location of the Muses Sea smooth terrain, including the first touchdown site on Itokawa. All images were taken in v-band (3). The square in (A) indicates the size of (B); the rectangle in (B) indicates the size of (C); the rectangle in (C) indicates the size of (D). Scale bars in (C) and (D), 1 m.

Itokawa is 550 m by 298 m by 224 m in its circumscribed box size .

Kaguya family

Possible lava tubes of the Moon

J. Haruyama et al., "Possible lunar lava tube skylight observed by SELENE cameras", *Geophysical Research Letters*, 2009.)

Figure 1. Images of a possible 65 m diameter lunar lava tube skylight in the Marius Hills taken by SELENE Terrain

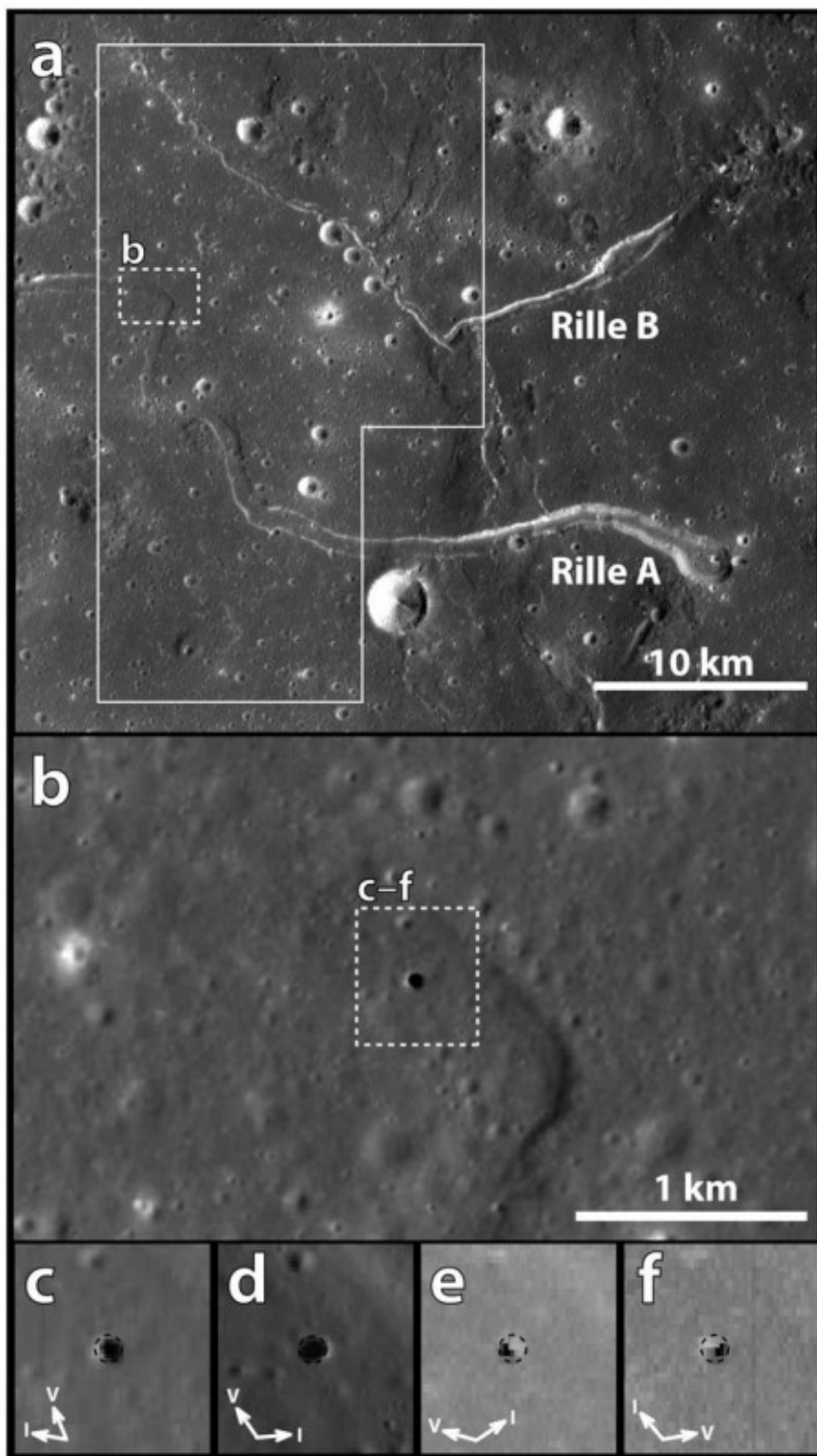
Camera (TC) and Multi-band Imager (MI). (a) Overview of the region (TC, 20 May 2008). The crater counting area is

indicated by a solid white polygon. (b) Marius Hills Hole (MHH) at 303.3E, 14.2N. (c – f)

Enlarged TC and MI images of MHH (Figures 1c and 1d are TC images from 20 May 2008 and 21 January 2009; Figures 1e and 1f are MI images

from 17 March 2009 and 13 April 2009). See Table 1 for imaging conditions. Arrows indicate the directions of solar

illumination (I) and the view vector from the camera (V).



Kaguya family

: Farside Gravity Field of the Moon

(N. Namiki et al., "Far-side Gravity Field of the Moon from Four-way Doppler Measurements of SELENE (Kaguya)", SCIENCE VOL 323, 2009.)

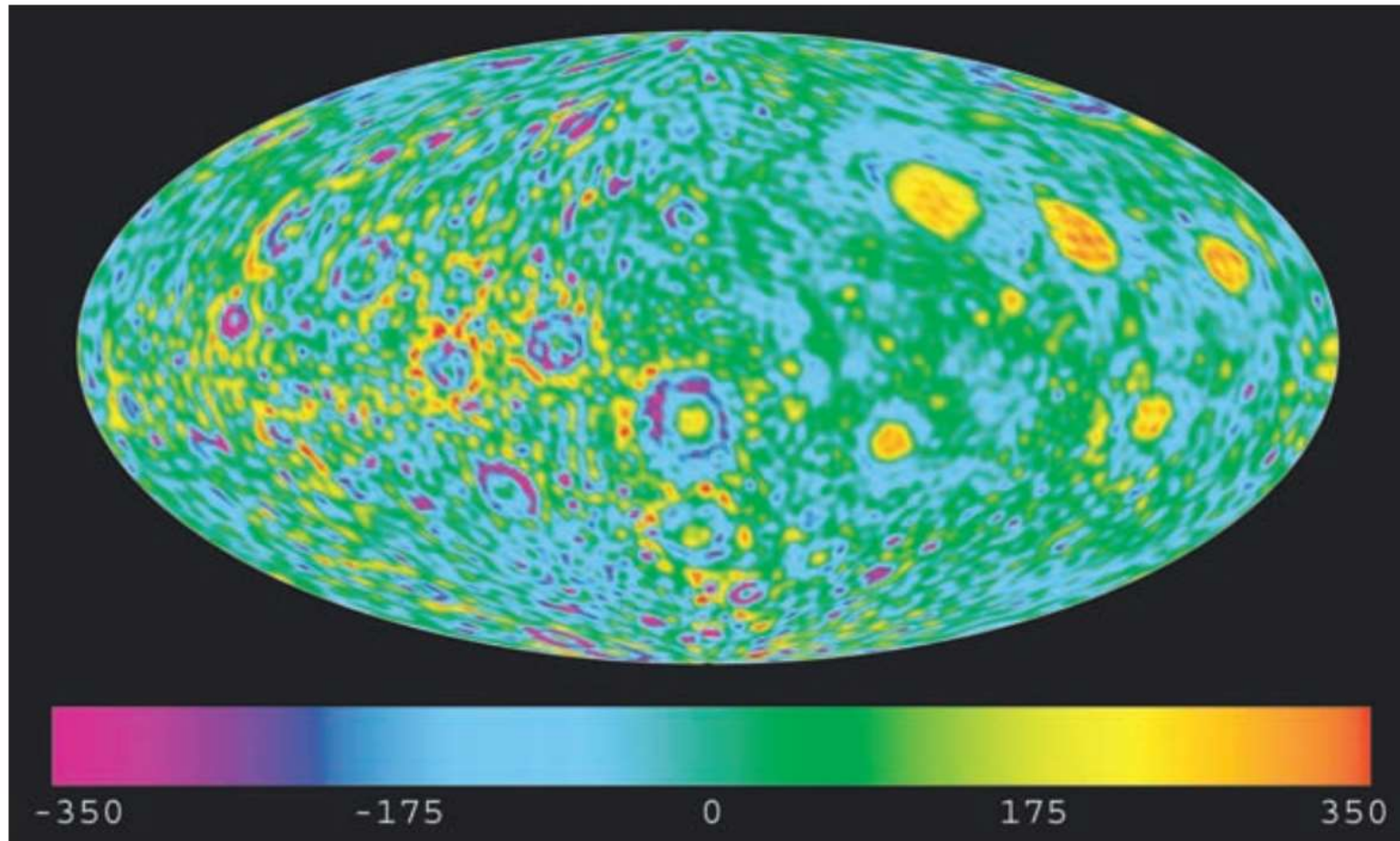


Fig. 2. Free-air gravity anomaly map from SGM90d. The lunar nearside is on the right side of the figure, and the farside is on the left. The color bar indicates the gravity anomaly in milliGalileo ($1 \text{ mGal} = 10^{-5} \text{ m s}^{-2}$). The maximum and minimum values of the map are 640 and -720 mGal .

Venus Express and Akatsuki Imamura et al 2018 JGR Radio Holography

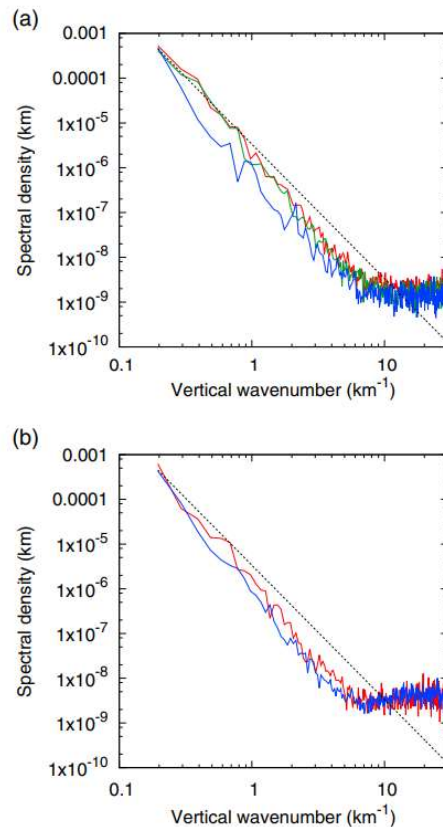


Figure 6. Vertical wavenumber spectra of the fractional temperature fluctua-

of the transition from the -3 power law to the noise floor, ~ 7 /km, corresponds to a wavelength of $\lambda_z \sim 150$ m, which is considered as the vertical resolution. To suppress noise without smoothing out meaningful structures, we have applied a 50-m-width smoothing to the profiles in Figure 5. This high vertical resolution enables FSI to resolve structures with a vertical scale of several hundred meters (Figure 5).

The measured temperature fluctuation is underestimated to some extent due to horizontal smoothing along the raypath. Ignoring the bending of the ray, the length of horizontal averaging H is estimated as (Kursinski et al., 1997)

$$H = 2\sqrt{(R+d)^2 - R^2} \sim 90 \text{ km}, \quad (3)$$

where $R = 6,122$ km corresponds to the altitude of 70 km, and the thickness of the atmospheric layer d is represented by the vertical resolution, which is taken to be 150 m in this study. The length H is regarded as the horizontal resolution of the measurement and is comparable to the horizontal wavelengths of the wave features observed in cloud images (e.g., Peralta et al., 2008). Considering such smoothing along the raypath, it is probable that the observed near-neutral layers represent localized turbulent neutral layers and that the static stabilities in those layers were measured to be slightly positive due to horizontal smoothing. It should be noted that the horizontal smoothing effect depends on the direction of the wavefront relative to the radio raypath; the wave amplitude can be largely correctly observed when the wavefront is parallel to the radio raypath, while the wave amplitude can be significantly underestimated when the wavefront is perpendicular to the raypath.

The influence of the noise in the measured signal phase on temperature retrieval was evaluated as follows. First, a linear function is fitted to the Doppler frequency time series, which is obtained by differentiating the phase, in the range outside the atmosphere. The noise component is extracted from this portion by subtracting the fitted function from the

with FSI in the altitude range of 65–75 km in different latitudinal regions obtained from (a) VeRa (blue: $<40^\circ$; green: $40^\circ - 70^\circ$; red: $>70^\circ$) and (b) Akatsuki RS (blue: $<40^\circ$; red: $>40^\circ$). The semiempirical spectrum for saturated gravity waves is also shown by dotted lines

Hayabusa2

小惑星探査機6年の旅

複数の小型探査ロボット, 小天体表面の移動探査
着陸精度 60 cm, 人工クレーター, 地下探査



Ref. ??? もしかして, はやぶさ1 ?

Hayabusa2

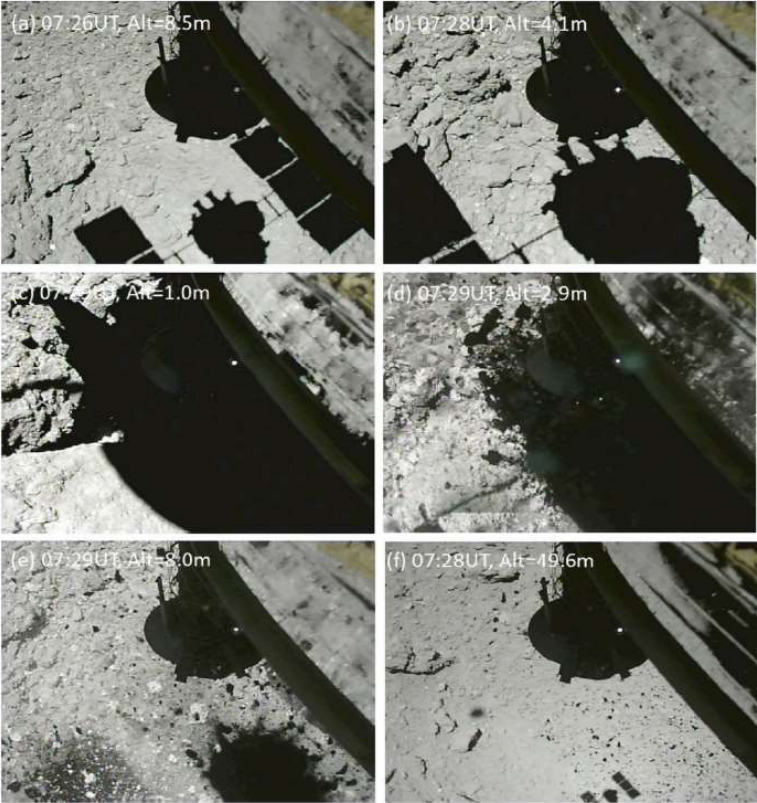
2020Tsuda Hayabusa2 mission status acta astronautica

新しいタブ × 2020Tsuda_Hayabusa2 mission st ×

ファイル | C:/Users/takano/Desktop/2.%20応用科学研究の論文/はやぶさ2 selected/2020Tsuda_Hayabusa2%20mission%20status_acta... ☆

手描き | Copilot に質問する | 9 / 13

Y. Tsuda, et al. Acta Astronautica 171 (2020) 42-54



(a) 07:26UT, Alt=8.5m (b) 07:28UT, Alt=4.1m
(c) 07:28UT, Alt=1.0m (d) 07:29UT, Alt=2.9m
(e) 07:29UT, Alt=3.0m (f) 07:28UT, Alt=19.6m

Fig. 13. A series of images captured by CAM-H before (a–c) and after (d–f) the touchdown.

検索 | 15:00 2024/07/06

Fig. 13. A series of images captured by CAM-H before (a–c) and after (d–f) the touchdown.

Fig..

Fig..

Fig..

Fig..

Fig..

Fig..